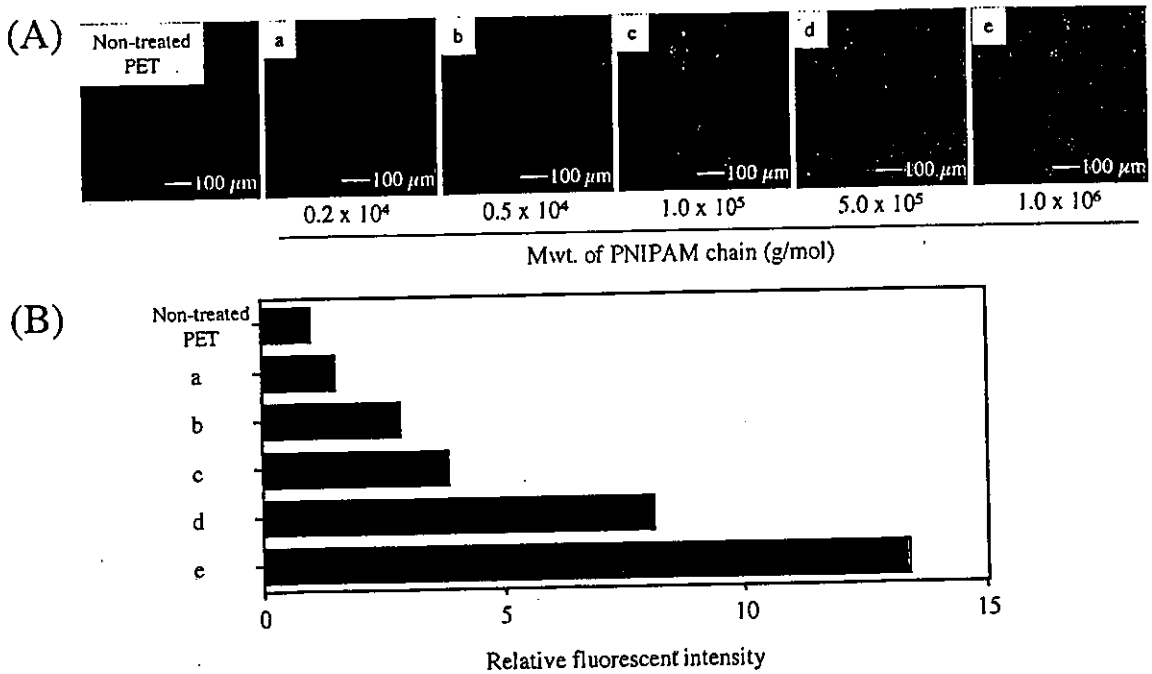

Figure 6. Complexation of PNIPAM–heparin with ATIII. (A) Fluorescence images measured by the CLSM, as a function of the mol wt of the PNIPAM chain in PNIPAM–heparin (after treatment with albumin as a blocking agent followed by ATIII, chromogenic staining using an ABC kit was performed). (B) The relative fluorescence intensity as a function of the mol wt of the PNIPAM chain in PNIPAM–heparin (the fluorescence intensity of the nontreated PET film is used as a control).

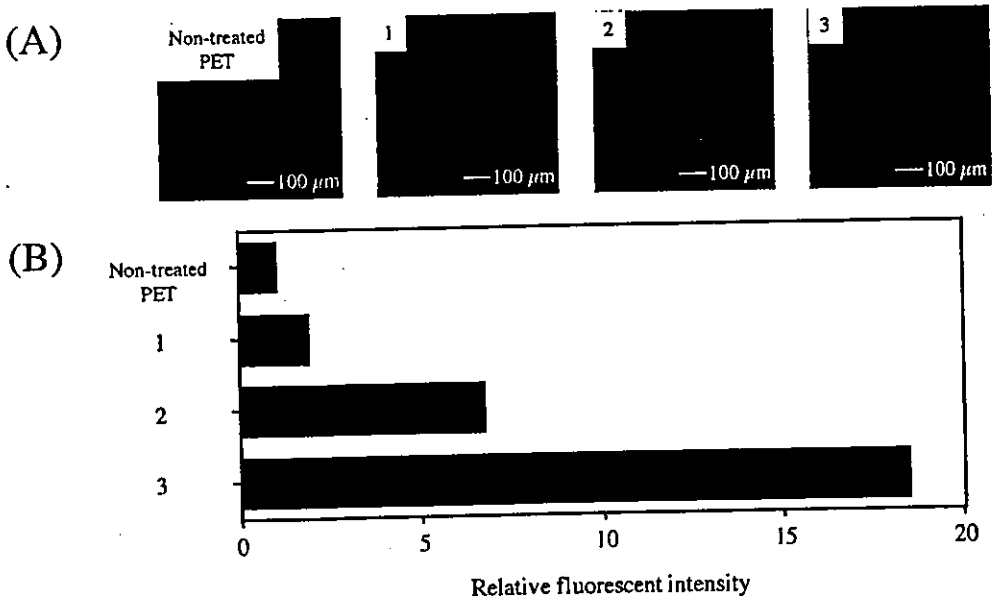

Figure 7. ATIII complexation capacity vs treatment temperature (mol wt of PNIPAM chain in PNIPAM–heparin: 1×10^4). The PET film, which is immersed in an aqueous solution containing PNIPAM–heparin, was incubated at either 20 or 40 °C (adsorption temperature) and then washed with water at either 20 or 40 °C (desorption temperature). Prior to adsorption of ATIII and ABC-kit treatment, albumin blocking treatment was performed. Adsorption and desorption temperatures are 20 and 20 °C for c1, 40 and 20 °C for c2, and 40 and 40 °C for c3, respectively. (c1, c2, c3 are referred to Table 2.)

containing buffer solution for blocking to avoid undesirable adsorption of proteins used for following successive procedures, subsequent immersion into the ATIII-containing buffer solution, and then treatment using the ABC kit as described above, as shown in Figure 7A. Note that the fluorescence intensities for nontreated PET film and the ATIII-free sample were very small. When the temperature for both adsorption and desorption was 20 °C, only a slight increase in the fluorescence intensity was noted as compared with the nontreated PET film surface as a control, whereas in the case of the adsorption temperature of 20 °C and desorption temperature of 40 °C, an almost 6-fold increase in the fluorescence intensity was noted (Figure 7B). When the temperature at both steps was 40 °C, a very high fluorescence intensity (almost 18 times higher than that of the control) was observed. Such film was also incubated in serum-containing medium (DMEM with 10% FCS) for 1 h. There was little difference in the fluorescence intensity before and after incubation. These results strongly indicate that the amount of adsorbed PNIPAM–heparin mainly depends on the temperature at the treatment steps; that is, when the treatment temperature was lower than LCST, desorption of PNIPAM–heparin was predominant, and when the temperature was higher than LCST, very high stability even in the serum-containing medium was noticed.

Discussion

Thermoresponsive polymer systems with LCST of approximately the physiological temperature range have received considerable attention in the biomedical field where the temperature-induced sol-to-gel transformation or phase transition phenomenon plays a significant role in biomedical functioning.[19] For example, thermoresponsive polymeric systems have been used in drug delivery matrixes,[20] cell sheet detachable two-dimensional (2D) cell substrate matrixes,[21,22] and three-dimensional (3D) cell-entrapping artificial extracellular matrixes[23,24] for tissue-engineering devices, in wound-healing matrixes for hemostasis,[25] and as tissue adhesion prevention material.[19] These are realized by utilizing a thermoresponsive physical phase transformation such as sol-to-gel or gel-to-sol transformations, depending on the type of application.

Thermoresponsiveness has been induced by incorporating a polymeric unit with LCST at an approximately physiological temperature into a designed material. To this end, the NIPAM monomer unit has been often used since the LCST of PNIPAM is approximately 32 °C. The present study showed that PNIPAM-conjugated heparin exhibited a thermoresponsive behavior such as solubilization or precipitation in the aqueous phase and adsorption or desorption at the water/substrate interface. Behavioral control would require precise control of the mol wt of PNIPAM, as indicated in this study. That is, complete precipitation above LCST in an aqueous solution and a strong adsorption characteristic were attained with higher-mol-wt PNIPAM (Figure 1). Control of the mol wt of PNIPAM was realized by iniferter photopolymerization, which was originally developed by Otsu et al. in the early 1980s.[14] The unique feature of this iniferter photopolymerization is that it proceeds in a quasi-living polymerization manner, in which "active" and "dormant" propagating chain ends are reversibly equilibrated under UV irradiation. This enables minimal transfer or termination reactions if an appropriate reaction condition is well selected. In our previous studies,[16-20] we developed iniferter-based graft-polymerized surfaces and block copolymers as surface coatings, both of which were designed to realize biocompatible surfaces.

Using this technique, we synthesized heparin with an iniferter group at its terminus under defined mild conditions without substantial cleavage of backbone and side chains and initiated living polymerization of NIPAM as schematically shown in Scheme 1. The resultant PNIPAM–heparin has LCST in an aqueous solution. LCST and complete or partial precipitation above LCST depended on the mol wt of PNIPAM: an increase in the mol wt of the graft chain lowered LCST. The stability of adsorbed PNIPAM–heparin on polymer films was higher at 40 °C than at 20 °C as evidenced by its wettability and surface chemical compositions (Figures 2–5). Although there was a small wettability difference with an increase in the mol wt of PNIPAM (Figure 2A), the surface coverage estimated from the surface chemical composition (Figure 2B) was enhanced with a higher mol wt of PNIPAM. The high-resolution analysis of subpopulations of C_{1s} and O_{1s} spectra clearly demonstrated the thermoresponsive adsorption and desorption and its graft chain mol wt dependency and substrate dependency (Figures 2–5). A higher mol wt graft chain and a highly hydrophobic surface such as PST enhanced surface adsorption at 40 °C and reduced desorption at 20 °C. These results indicate that a hydrophobic interaction-driven process is dominant. In fact, for hydrophobic PST, there appears little desorption at 20 °C when PNIPAM–heparin with a high mol wt graft chain is employed (Figure 4 and Table 3).

The degree of complexation with ATIII, which determines the degree of anticoagulation, was also significantly enhanced with a higher mol wt of PNIPAM (Figure 3). This means that higher-mol-wt PNIPAM enhances the adsorption of heparin (higher adsorption capability and less desorption capability than those of lower-mol-wt PNIPAM).

In addition to the amount of PNIPAM–heparin adsorbed on the film surface, the configuration of PNIPAM–heparin is also considered as a determinant of anticoagulation activity: the ideal configuration is that the PNIPAM segment is anchored on the surface and the heparin molecule is oriented vertically in the aqueous phase, thus facilitating complexation with ATIII at a physiological temperature. This configuration is best suited for surface heparinization without substantial loss of the biological activity of heparin, as proposed and verified by Olsson's end-point attachment of the heparin molecule via the surface-coupling approach,[7] our alkylated heparin as a heparin surfactant via the surface adsorption approach,[12] and the biomimetic engineered glycolyx-like surface approach using oligosaccharide surfactant polymers developed by Marchant et al.[26] Marchant's oligosaccharide surfactant polymers consisted of flexible poly(vinylamine) with dextran and alkanoyl side chains. They demonstrated that alkanoyl side groups self-assemble on the hydrophobic surface via epitaxial adsorption, the main chains lie parallel to the surface, and solvated oligosaccharide side chains protrude into the aqueous phase, creating a glycocalyx-like coating. The resulting biomimetic surface is effective in suppressing protein adsorption and adhesion.

Taken together with this evidence, it can be said that bioconjugation of bioactive heparin and PNIPAM having a thermally induced phase transition characteristic provides a thermoresponsive surface biocompatible coating via adsorption and precipitation. Although we have not evaluated the anticoagulant activity of PNIPAM–heparin as a thermoresponsive biocompatible coating on an extracorporeal circuit, treatment of the entire blood-contacting surface of a device with an aqueous solution containing with PNIPAM–heparin at room temperature and subsequent elevation of temperature to a physiological temperature may provide a heparinized surface on which the heparin molecule is exposed to the fluid phase and the precipitated PNIPAM segment is anchored on the surface of the extracorporeal device, which appears to resist replacement with hydrophobic plasma components. In fact, the incubation of PNIPAM–heparin-treated film in the serum-containing medium did not induce the significant change in surface biological activity as mentioned above; this results in the maintenance of antithrombogenicity at least for a short-term extracorporeal circulation.

(18) Kidoaki, S.; Nakayama, H.; Matsuda, T. *Langmuir* **2001**, *17*, 1080–1087.
(19) Ohya, S.; Nakayama, Y.; Matsuda, T. *Biomacromolecules* **2001**, *2*, 856–863.
(20) Miura, M.; Cole, C.-A.; Monji, N.; Hoffman, A. S. *J. Biomater. Sci., Polym. Ed.* **1994**, *5*, 555–568.
(21) Takezawa, T.; Yamazaki, M.; Mori, Y.; Yonaha, T.; Yoshizato, K. *J. Cell Sci.* **1992**, *101*, 495–501.
(22) Okano, T.; Yamada, N.; Sakai, H.; Sakurai, Y. *J. Biomed. Mater. Res.* **1993**, *27*, 1243–1251.
(23) Matsuda, T.; Moghaddam, M. J. *Mater. Sci. Eng.* **1993**, *C1*, 37–43.
(24) Moghaddam, M. J.; Matsuda, T. *ASAIO Trans.* **1991**, *37*, 437–438.
(25) Morikawa, N.; Matsuda, T. J. *Biomat. Sci.*, in press.
(26) Holland, N. B.; Qui, Y.; Ruegsegger, M.; Marchant, R. E. *Nature* **1998**, *39*, 799–801.

In conclusion, PNIPAM–heparin is a thermoresponsive biocompatible coating material. The adsorption and stability of adsorbed PNIPAM–heparin were enhanced with an increase in the mol wt of PNIPAM. Simultaneously, complexation of heparin with ATIII was enhanced. Desorption was facilitated by decreasing the temperature of water and by using polar surfaces such as PET and PU. We have not yet investigated how such a temperature-induced "switching on and off" of anticoagulant activity functions well in vivo, but we are planning to verify such biofunctioning using a minicolumn simulating extracorporeal circulatory device. Thus, it can be concluded that the combination of thermoresponsive PNIPAM and bioactive heparin provides a unique feature for use in biocompatible coatings.

Acknowledgment. This study was financially supported by the Promotion Fundamental Studies in Health Science of the Organization for Pharmaceutical Safety and Research (OPSR) under Grant No. 97-15 and in part by a Grant-in-Aid for Scientific Research (A2-12358017, B2-12470277) from the Ministry of Education, Culture, Sports, Science, and Technology of Japan.

LA011408S

Journal of Cardiovascular Pharmacology™
39:784–788 © 2002 Lippincott Williams & Wilkins, Inc., Philadelphia

Reprinted from JOURNAL OF CARDIOVASCULAR PHARMACOLOGY
Vol. 39, No. 6 June 2002
Lippincott Williams & Wilkins Printed in U.S.A.

Local Delivery of Single Low-Dose of C-Type Natriuretic Peptide, an Endogenous Vascular Modulator, Inhibits Neointimal Hyperplasia in a Balloon-Injured Rabbit Iliac Artery Model

Satoshi Yasuda, Masahiko Kanna, Satoru Sakuragi, Sunao Kojima, Yasuhide Nakayama, Shunichi Miyazaki, *Takehisa Matsuda, Kenji Kangawa, and Hiroshi Nonogi

*National Cardiovascular Center, Osaka, Japan, and *Kyushu University School of Medicine, Fukuoka, Japan*

Summary: C-type natriuretic peptide (CNP) is an endogenous vascular modulator. In addition to vasodilation, CNP exerts multifunctions including anti-thrombus and anti-proliferation actions against vascular smooth muscle cells and myofibroblasts. Therefore, CNP is a potential therapeutic agent for the prevention of restenosis following angioplasty. The current study investigated whether local delivery of CNP, even at microgram levels about three orders of magnitude lower than doses (high milligram levels) used for systemic administration in the previous study, attenuates neointimal hyperplasia. The rabbit iliac artery was denuded, and then CNP (100 μg, n = 5) or control vehicle (n = 5) was administered locally over 20 min, via a local drug delivery catheter. During drug delivery, blood pressure was monitored with a high-fidelity micromanometer catheter. There was no significant decrease in arterial pressure immediately after the CNP administration. Four weeks after the treatment, computer-assisted morphometric analysis revealed significant reduction in the intimal area (CNP 0.44 ± 0.27 versus control 0.96 ± 0.20 mm^2, $p < 0.01$), but no changes in the medial area (CNP 0.93 ± 0.23 versus control 0.79 ± 0.29 mm^2, p = NS). This resulted in a significant decrease in the ratio of the intimal area to the medial area in CNP-treated vessels compared with control vessels (CNP 0.45 ± 0.26 versus control 1.40 ± 0.66, $p < 0.05$). Local delivery of a single low dose of CNP effectively inhibits neointimal hyperplasia with a minimal likelihood of compromising hemodynamics. Considering its multipotent actions and its role as an important regulator of the vascular system, this treatment may have a therapeutic advantage for clinical use. **Key Words:** Angioplasty—Drugs—Natriuretic peptides—Pharamacology—Restenosis.

Received August 20, 2001; accepted November 29, 2001.
Address correspondence and reprint requests to Dr. Satoshi Yasuda at the Division of Cardiology, Department of Medicine, National Cardiovascular Center, Fujishirodai 5-7-1, Suita, Osaka, 565-8565, Japan. E-mail: syasuda@hsp.ncvc.go.jp

C-type natriuretic peptide (CNP) is the third member of the natriuretic peptide family and consists of 22 amino acids with a ring structure formed by intramolecular disulfide linkage (1). Endogenous CNP is secreted by vascular endothelial cells and functions as an important local vascular modulator through natriuretic peptide receptor-B (2). In addition to its vasodilatory properties (3), CNP exerts multiple effects, including inhibition of the proliferation of vascular smooth muscle cells (4) and myofibroblastic cells (5), acceleration of endothelialization (6), and regulation of thrombosis (7). These effects of CNP suggest a therapeutic potential in cardiovascular diseases such as in atherosclerosis and postangioplasty restenosis (8). In fact, in a rabbit carotid artery injury model (9), CNP infused IV for 14 consecutive days (total dose: high milligram levels) resulted in a significant inhibition of neointimal formation.

Recently, local administration of the drug directly to the target site has been increasingly attracting interest because of its several possible advantages (10,11). First, high local concentrations of the drug can be administered. Second, local dosing, without substantial systemic dosing, could prevent the occurrence of systemic adverse effects. Thus, in the current study, we investigated whether local delivery of a single low dose of CNP, even at microgram levels, attenuates neointimal hyperplasia, which occurs in rabbits in response to vascular injury.

METHODS

All of the procedures were in accordance with the institutional guidelines, which conform to the "Position of the American Heart Association on Research Animal Use."

The model

New Zealand white rabbits weighing 3.0–3.5 kg were used for this study as in our previous study (12). Anesthesia was induced by IM injection of ketamine (50 mg/kg body weight), following treatment with xylazine (10 mg/kg body weight). The right femoral arteries were exposed by an incision below the inguinal ligament. Heparin sulfate (1,000 U) was administered IV to prevent blood coagulation. After administration of 2 ml of 1% lidocaine, a 3.6 Fr angioplasty catheter (Tokai Medical Products, Inc., Aichi, Japan) (13) was introduced into the right iliac artery under fluoroscopic guidance by an over-the-wire system. This catheter (13) performs three functions consisting of balloon inflation, local drug administration, and blood perfusion and therefore enables drug delivery over a relatively long duration (over 20 min) while maintaining perfusion. The 3.0-mm-diameter, 20-mm-long balloon was inflated with a contrast medium at the right iliac artery immediately distal to the aortic bifurcation (a reliable and reproducible landmark for the removal of arterial vessels at a later date). The balloon inflated at a pressure of 6 atm and was then retracted and deflated. This procedure was repeated three times in the same segment (20 mm in length from the bifurcation) to ensure complete endothelial denudation. In the current study, 10 rabbits were subjected to the balloon injury.

Local delivery of C-type natriuretic peptide

Following the balloon-induced injury, the drug was locally delivered via a multifunctional angioplasty catheter. This device was described in detail in our previous reports (12,13). Briefly, the drug delivery port was positioned at the injured site and the balloon was inflated at a low pressure (2 atm) to allow accumulation of the drug. Then the guidewire was moved to a site proximal to the perfusion port to allow distal perfusion. In pilot studies using this device (13), the drug permeated into the medial tissues and the adventitia immediately after the local delivery. The drug then persisted in the media for at least 24 h. Using an infusion pump (STC-521, Terumo, Japan), 100 μg of CNP (gift of Dr. Kangawa, Research Institute, National Cardiovascular Center, Osaka, Japan) was locally administered to the rabbits dissolved in 10 ml of saline (CNP group, $n = 5$) or a vehicle solution without CNP (control group, $n = 5$) over 20 min via the local drug delivery catheter. The dose of CNP used in the current study was about three orders of magnitude lower than the doses (50–100 mg) used for systemic administration in a previous study in rabbits (9).

Hemodynamic measurements

In four rabbits under anesthesia, a 1.4 Fr high-fidelity micromanometer catheter (Miller Instruments, Houston, TX, U.S.A.) was inserted into the abdominal aorta via the left femoral artery. The systemic arterial pressure and heart rate were continuously recorded using a polygraph (model RA 1000, NEC San-ei Instruments, Ltd., Tokyo, Japan) at 5-min intervals during the 20-min local delivery of CNP. Measurements were continued until 20 min after the treatment. Ten sequential heart rates were averaged at each time point.

Postmortem procedures

On the 28th day after the procedure, the rabbits were killed by injection of a fatal dose of pentobarbital. For pressure perfusion fixation, a midabdominal incision was made and the lower abdominal aorta was isolated,

flushed with saline, and fixed with 10% buffered formalin at 80 mm Hg for > 15 min. At least 24 h after fixation, the arterial segments were dehydrated and embedded in paraffin (12).

Data and statistical analyses

For histology, 5-μm sections were cut and stained with elastin van Gieson. Morphometric analysis of arterial cross-sections was performed on the 28th day after the local delivery and cross-sections were imaged using a National Institutes of Health image software package. The endoluminal border, the circumference bounded by the internal elastic lamina, and the external elastic lamina were manually traced, and then the luminal, intimal, and medial areas were calculated. The results in all segments (three to five different cross-sections of each of the proximal, middle, and distal lesions from the aortic bifurcation) within a single artery were averaged. We compared aforementioned parameters between the control and the CNP-treated vessels.

All data were expressed as mean ± SD. To compare the CNP-treated vessels with the control vessels, data were analyzed using the unpaired Student's *t* test to evaluate the two-tailed levels. In rabbits treated with CNP, the hemodynamics data were compared by analysis of variance. A value of $p < 0.05$ was considered as denoting significant difference.

RESULTS

To evaluate acute systemic effects of local delivery of CNP, hemodynamics were measured in four rabbits with a systolic blood pressure of 75 ± 18 mm Hg and a heart rate of 192 ± 12 beats/min as the baseline. Figure 1 shows the fold changes in systolic blood pressure compared with the baseline level. There was no significant decrease in systemic blood pressure during and after the treatment with CNP (0.96-fold ± 0.10-fold change). The heart rate did not change significantly throughout the study either (1.02-fold ± 0.10-fold change). These findings indicate that the local delivery of CNP at a low dose is minimally associated with compromising hemodynamics.

Table 1 summarizes the morphometric data on the 28th day after the administration for both groups. Local delivery of 100 μg of CNP induced a significant reduction in the intimal area, but no change in the medial area was observed. This resulted in a significant decrease in the ratio of the area of the intima to that of the media in the CNP-treated vessels compared with the control vessels, indicating attenuation by CNP of neointimal hyperplasia that occurred in response to the balloon injury. Figure 2 shows representative micrographs of cross-sections of the injured arterial segments on the 28th day after the treatment.

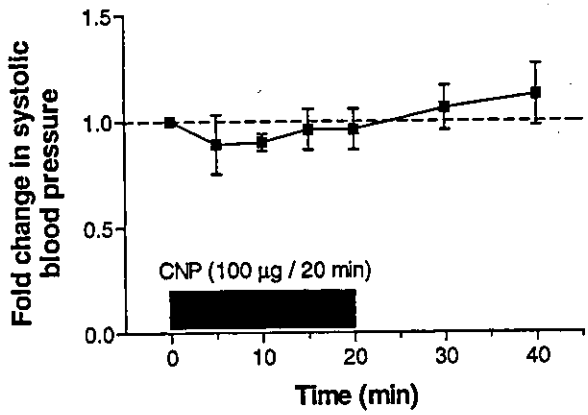

FIG. 1. Changes in systolic blood pressure (measured using a high-fidelity micromanometer catheter) during and after local delivery of 100 μg of C-type natriuretic peptide (CNP) in 4 rabbits. The points are mean ± SD of the fold change compared with the baseline level (by definition, 1.0-fold before drug delivery).

DISCUSSION

An important finding of this study is that local delivery of a single low dose of CNP effectively inhibits neointimal hyperplasia without the systemic adverse effect of hypotension.

CNP is produced locally in the vessels (2) and plays an important role as an endogenous vascular modulator that is involved in many events to regulate vascular tone and growth (3,8). CNP is potently anti-mitogenic for vascular smooth muscle cells, in which the natriuretic peptide receptor-B is preferentially expressed (4,14). Inhibition of proliferation is observed in other cell types such as myofibroblasts (5) and fibroblasts (15), both of which are

TABLE 1.

Comparison of arterial morphometry on the 28th day after the local delivery of C-type natriuretic peptide

	100 μg CNP (n = 5)	Control (n = 5)
Intimal area, mm^2	0.44 ± 0.27[a]	0.96 ± 0.20
Medial area, mm^2	0.93 ± 0.23	0.79 ± 0.29
Intimal-to-medial area ratio (%)	0.45 ± 0.26[a]	1.40 ± 0.66

CNP, C-type natriuretic peptide.
Values are mean ± SD.
[a]$P < 0.05$ vs. control.

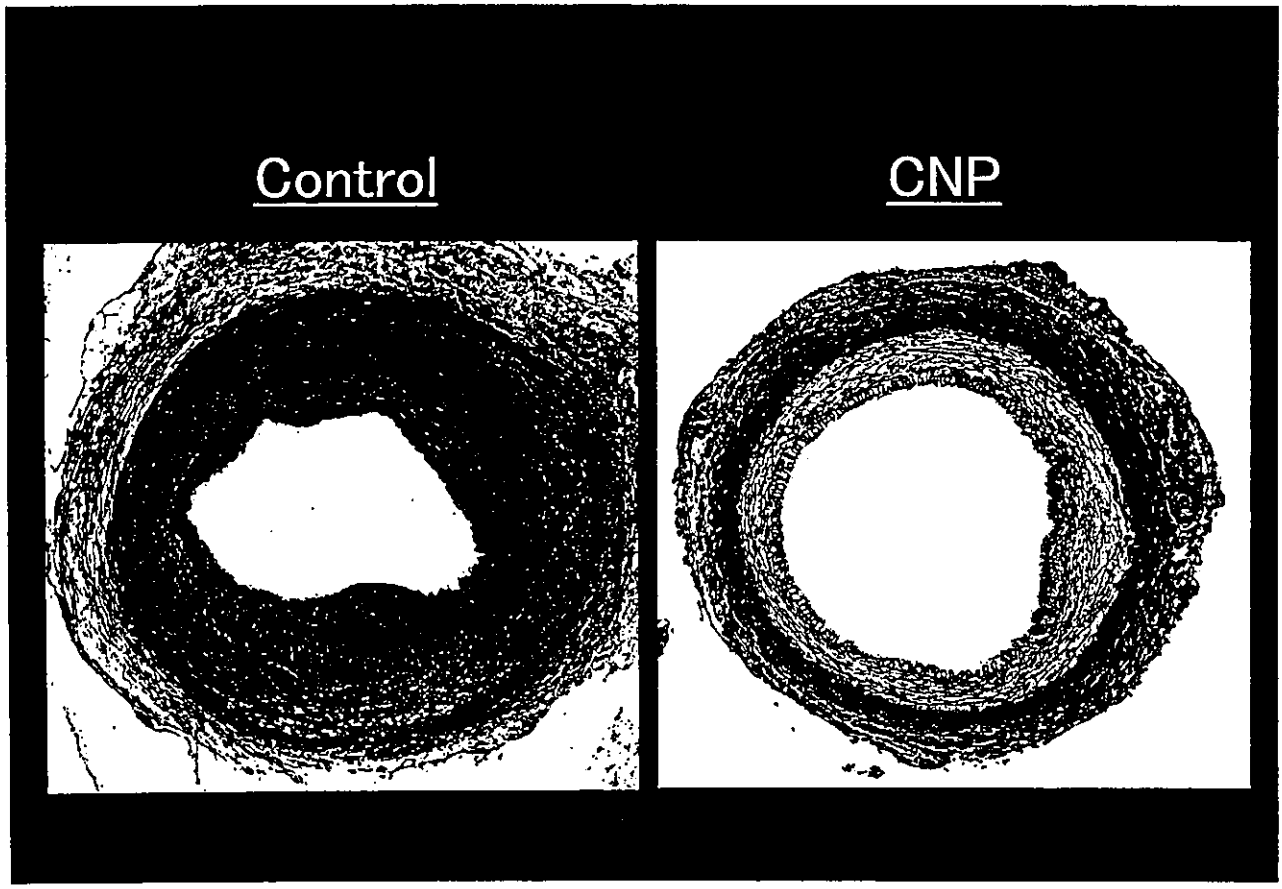

FIG. 2. Cross-section (elastin van Gieson stain, ×40) of rabbit iliac arteries on the 28th day after balloon injury. **Left panel.** Control artery. **Right panel.** C-type natriuretic peptide (CNP) (100 μg)-treated artery. Note marked inhibition of intimal hyperplasia in CNP-treated artery.

key players in the process of vascular remodeling (16). Moreover, recent studies have shown that CNP may promote endothelialization (6) and regulate thrombosis (7). These characteristics of CNP as a multifunctional peptide could exert a great effect in the treatment of atherosclerosis and postangioplasty restenosis because complicated mechanisms involving many factors underlie the progression of these diseases.

The present study has demonstrated that the local delivery of 100 μg of CNP significantly inhibited neointimal hyperplasia, as shown in Table 1 and Figure 2. This inhibition was achieved after a single administration at microgram levels only, which was about three orders of magnitude lower than doses used for systemic administration (14 consecutive days) in the previous study in rabbits (9), indicating a high efficacy of the local drug delivery (10,11).

CNP has a vasodilatory action, although it is modest compared with that of the atrial natriuretic peptide (8). Therefore, we also evaluated acute systemic effects of local delivery of CNP on hemodynamics using a high-fidelity micromanometer catheter. Neither the blood pressure (Fig. 1) nor the heart rate changed, indicating another advantage (a minimal likelihood of systemic adverse effects) of this method.

Previous experimental studies showed that adenovirus-mediated CNP gene transfer prevented vascular constrictive remodeling (17) and neointimal hyperplasia (18). In contrast to these gene therapies, active CNP is present at the time of injury in the current study, possibly targeting early events important for restenosis, including the recruitment of preexisting, circulating smooth muscle progenitor cells (19). Administration of CNP may also supply endogenous production that is decreased in endothelium-denuded vessels, which may be of help to maintain the vascular physiology.

With respect to clinical implications, issues regarding potential inflammatory effects of adenoviral vectors warrant consideration (20). Currently, the catheter-based peptide delivery or CNP-coated bioactive stents may be

of more practical use for patients. Further studies are needed to determine the effects of CNP administration on atherosclerotic vessels, which would advance the present method. In conclusion, considering its multipotent actions and its role as an important endogenous regulator in the vascular system, local delivery of vasoactive CNP may have a therapeutic advantage for clinical use.

Acknowledgments: This study was supported in part by the Promotion of Fundamental Studies in Health Science of the Organization for Pharmaceutical Safety and Research of Japan, Tokyo, Japan.

REFERENCES

1. Sudoh T, Minamino N, Kangawa K, et al. C-type natriuretic peptide (CNP): a new member of natriuretic peptide family identified in porcine brain. *Biochem Biophys Res Commun* 1990;168:863–70.
2. Komatsu Y, Nakao K, Itoh H, et al. Vascular natriuretic peptide. *Lancet* 1992;340:622.
3. Stingo AJ, Clavell AL, Aarhus LL, et al. Cardiovascular and renal actions of C-type natriuretic peptide. *Am J Physiol* 1992;262:H308–12.
4. Furuya M, Yoshida M, Hayashi Y, et al. C-type natriuretic peptide is a growth inhibitor of rat vascular smooth muscle cells. *Biochem Biophys Res Commun* 1991;177:927–31.
5. Tao J, Mallat A, Gallois C, et al. Biological effects of C-type natriuretic peptide in human myofibroblastic hepatic stellate cells. *J Biol Chem* 1999;274:23761–9.
6. Doi K, Ikeda T, Itoh H, et al. C-type natriuretic peptide induces redifferentiation of vascular smooth muscle cells with accelerated re-endothelialization. *Arterioscler Thromb Biol* 2001;21:930–6.
7. Yoshizumi M, Tsuji H, Nishimura H, et al. Natriuretic peptides regulate the expression of tissue factor and PAI-1 in endothelial cells. *Thromb Haemost* 1999;82:1497–503.
8. Chen HH, Burnett JC. C-type natriuretic peptide: the endothelial component of the natriuretic peptide system. *J Cardiovasc Pharmacol* 1998;32(suppl 3):S22–8.
9. Shinomiya M, Tashiro J, Saito Y, et al. C-type natriuretic peptide inhibits intimal thickening of rabbit carotid artery after balloon catheter injury. *Biochem Biophys Res Commun* 1994;205:1051–6.
10. Lincoff AM, Topol EJ, Ellis SG. Local drug delivery for the prevention of restenosis: fact, fancy, and future. *Circulation* 1994;90:2070–84.
11. Ettenson DS, Edelman ER. Local drug delivery: an emerging approach in the treatment of restenosis. *Vasc Med* 2000;5:97–102.
12. Yasuda S, Noguchi T, Gohda M, et al. Single low-dose administration of human recombinant hepatocyte growth factor attenuates intimal hyperplasia in a balloon-injured rabbit iliac artery model. *Circulation* 2000;101:2546–9.
13. Noguchi T, Yasuda S, Itoh T, et al. New multifunctional percutaneous transluminal coronary angioplasty catheter device capable of balloon inflation, local drug delivery and coronary perfusion. *J Cardiol* 2000;35:41–5.
14. Furuya M, Tawaragi Y, Minamitake Y, et al. Structural requirements of C-type natriuretic peptide for elevation of cyclic GMP in cultured vascular smooth muscle cells. *Biochem Biophys Res Commun* 1992;183:964–9.
15. Chrisman TD, Garbers DL. Reciprocal antagonism coordinates C-type natriuretic peptide and mitogen-signaling pathways in fibroblasts. *J Biol Chem* 1999;274:4293–9.
16. Scott NA, Cipolla GD, Ross CE, et al. Identification of a potential role for the adventitia in vascular lesion formation after balloon overstretch injury of porcine coronary arteries. *Circulation* 1996 93:2178–87.
17. Morishige K, Shimokawa H, Yamawaki T, et al. Local adenovirus-mediated transfer of C-type natriuretic peptide suppresses vascular remodeling in porcine coronary arteries in vivo. *J Am Coll Cardiol* 2000;35:1040–7.
18. Ueno H, Haruno A, Morisaki N, et al. Local expression of C-type natriuretic peptide markedly suppresses neointimal formation in rat injured arteries through an autocrine/paracrine loop. *Circulation* 1997;96:2272–9.
19. Saiura A, Sata M, Hirata Y, et al. Circulating smooth muscle progenitor cells contribute to atherosclerosis. *Nat Med* 2001;7:382–3.
20. DeYoung MB, Dichek DA. Gene therapy for restenosis: are we ready? *Circ Res* 1998;82:306–13.

doi:10.1006/cyto.2002.1048, available online at http://www.idealibrary.com on IDEAL®

BIOMATERIAL SURFACE CHEMISTRY DICTATES ADHERENT MONOCYTE/MACROPHAGE CYTOKINE EXPRESSION IN VITRO

W. G. Brodbeck,[1] Y. Nakayama,[3] T. Matsuda,[4] E. Colton,[1] N. P. Ziats,[1,2] J. M. Anderson[1,2]*

An in vitro human monocyte culture system was used to determine whether adherent monocyte/macrophage cytokine production was influenced by material surface chemistry. A polyethylene terephthalate (PET) base surface was modified by photograft copolymerization to yield hydrophobic, hydrophilic, anionic and cationic surfaces. Freshly isolated human monocytes were cultured onto the surfaces for periods up to 10 days in the presence or absence of interleukin-4 (IL-4). Semi-quantitative RT-PCR analysis on days 3, 7 and 10 of cell culture revealed that interleukin-10 (IL-10) expression significantly increased in cells adherent to the hydrophilic and anionic surfaces but significantly decreased in the cationic surface adherent monocytes/macrophages. Conversely, interleukin-8 (IL-8) expression was significantly decreased in cells adherent to the hydrophilic and anionic surfaces. Further analysis revealed that the hydrophilic and anionic surfaces inhibited monocyte adhesion and IL-4–mediated macrophage fusion into foreign body giant cells (FBGCs). Therefore, hydrophilic and anionic surfaces promote an anti-inflammatory type of response by dictating selective cytokine production by biomaterial adherent monocytes and macrophages. These studies contribute information necessary to enhance our understanding of biocompatibility to be used to improve the in vivo lifetime of implanted medical devices and prostheses.

Biocompatibility of implanted medical devices and prostheses is determined by the host foreign body response to the surface of the implanted material. Immediately following implantation, the surface of the material is coated with plasma proteins that further direct cellular adhesion and activation. The inflammatory response ensues and monocytes migrate to the tissue/material interface and adhere to the protein-coated surface of the implant. Resolution of the inflammatory response and progression of wound healing coincide with differentiation of the biomaterial adherent monocytes into macrophages, which may further fuse to form foreign body giant cells (FBGCs).[1–6] Multinucleated foreign body giant cells are present on the surface of implants over their in vivo lifetimes[7] and are responsible for causing stress cracking and oxidative damage to the implant by concentrating phagocytic and degradative properties.[8,9] Short and long term surface-adherent macrophages participate in these events through the secretion of cytokines. Therefore, ways of modulating the presence and activity of biomaterial adherent macrophages and FBGCs and their overall response to the biomaterial surface are currently being sought and comprise an active area of research in surface modification.

Like most responses involving migratory immune cells, the events following implantation of prostheses are guided by cytokines. The modern classification of cytokines places them into Th_1 and Th_2 subgroups based on their effects of an immune response, promoting either a cellular or humoral mediated response, respectively. Th_1 cytokines include interleukin-1 beta (IL-1β), tumor necrosis factor-alpha (TNF-α) and interleukin-8 (IL-8), while Th_2 cytokines include

From the Departments of [1]Pathology and [2]Biomedical Engineering, Case Western Reserve University, Cleveland, Ohio, USA; [3]Department of Bioengineering, National Cardiovascular Center, Osaka, Japan; [4]Department of Biomedical Engineering, Kyushu University, Fukuoka, Japan

*Correspondence to: James. M. Anderson, MD, Ph.D., Institute of Pathology, Rm 306, Case Western Reserve University School of Medicine, Cleveland OH 44106, USA. Tel: 1-216-844-1020; Fax: 1-216-844-8004

E-mail: wgb2@po.cwru.edu (1st author)

Received 28 January 2002; received in revised form 14 May 2002; accepted for publication 23 May 2002

1043–4666/02/$-see front matter © 2002 Elsevier Science Ltd. All rights reserved.

KEY WORDS: biocompatibility/foreign body giant cell/inflammation/macrophage/wound healing

interleukin-6 (IL-6), interleukin 10 (IL-10) and interleukin-1 receptor antagonist (IL-1RA).

Alternatively, in terms of biomaterial biocompatibility, cytokines are described based upon their role in influencing the foreign body response to the implanted material, promoting either inflammation or wound healing. TNFα, IL-8 and IL-6 are considered pro-inflammatory/anti-wound healing cytokines due to their collective ability to promote inflammation by cellular activation and chemotaxis. Cytokines that inhibit the inflammatory response and promote wound healing such as IL-1RA are considered anti-inflammatory/pro-wound healing. IL-1β and IL-10 are two unique cytokines in this classification scheme since they represent the extremes of the responses. IL-1β is considered a pro-inflammatory/pro-wound healing cytokine due to its ability to activate both inflammatory cells (lymphocytes and monocytes) and wound healing cells (fibroblasts). IL-10 acts in the opposite fashion by down-regulating the activity of these cell types and suppressing further cytokine production leading to an anti-inflammatory/anti-wound healing effect.

One of the main sources of cytokines at the tissue/implant interface is the adherent monocyte/macrophage population. The cytokines produced by these cells during the early stages of the foreign body reaction (within the first 2 weeks following implantation) influence the recruitment and activation of other leukocytes (namely neutrophils and lymphocytes). Neutrophils can induce biomaterial surface damage by generating degradative products through the respiratory burst, while lymphocytes interact with adherent monocyte-derived macrophages to amplify local inflammatory or wound healing cytokine concentrations. Additionally, IL-4 and IL-13 produced by CD4+ T cells induce the fusion of macrophages into FGBCs[4,10,11] leading to the degradation of the biomaterial surface and failure of the implant. Therefore, controlling the local cytokine milieu is essential for promoting the desired response.

A possible method of controlling biomaterial adherent monocyte/macrophage cytokine expression is through the modification of surface/substrate chemistry. The protein layer adsorbed to the surface of a biomaterial implant is dependent upon the surface chemistry,[12,13] which can determine the degree of monocyte and macrophage adhesion. Similarly, the protein layer also influences the activation of these cells and the types and levels of secreted cytokines by engagement of monocyte/macrophage cell surface receptors to the appropriate ligands. This biomaterial-dependent cytokine expression has been previously described when examining secretion of IL-1β, IL-6, TNF-α and IL-1RA by adherent macrophages.[14–16] Therefore, biomaterial surface chemistry directly or indirectly dictates monocyte adhesion, and macrophage activation and fusion by determining the types, levels and conformations of adsorbed proteins.

For these studies, we used our previously established in vitro human monocyte culture system and semi-quantitative RT-PCR to determine whether biomaterial surfaces displaying distinct surface chemistries influence adherent monocyte/macrophage expression of IL-1β, IL-1RA, TNF-α, IL-6, IL-8 and IL-10 and whether this influence would promote either inflammatory or wound healing responses. The surfaces tested consisted of poly(benzyl *N,N*-diethyldithiocarbamate-co-styrene) (BDEDTC), polyacrylamide (PAAm), sodium salt of poly(acrylic acid) (PAANa) and methiodide of poly(dimethylaminopropyl-acrylamide) (DMAPAAmMeI), which provided hydrophobic, hydrophilic, anionic and cationic surface chemistries respectively. We found that PAAm and PAANa surfaces promote an anti-inflammatory response by promoting an increased IL-10 production and decreased IL-8 production by biomaterial adherent human monocytes and macrophages. In cultures where recombinant IL-4 was added to promote macrophage fusion, cells adherent to the DMAPAAmMeI surface expressed decreased levels of IL-1RA and IL-10, promoting an inflammatory response. Therefore, biomaterial surface chemistry dictates the levels of cytokines produced by adherent monocytes and macrophages, having strong implications in the determination of biomaterial biocompatibility.

RESULTS

Monocyte/macrophage adhesion and fusion rates were determined for the surfaces tested. In agreement with our previous in vitro[17] and in vivo (unpublished observations) studies, PAAm and PAANa surfaces promoted significantly decreased levels of monoycyte/macrophage adhesion ($P \leq 0.045$) and macrophage fusion ($P \leq 0.019$) when compared to the polyethylene terephthalate (PET) base surface (Fig. 1A and B, respectively). Macrophage fusion was significantly increased ($P \leq 0.003$ when compared to the PET base surface) on DMAPAAmMeI surfaces when cultured in the presence of IL-4 on days 7 and 10, and in the absence of IL-4 on day 10.

Cytokine mRNA expression was quantitatively determined by semi-quantitative RT-PCR and values are expressed as expression ratios as determined by comparison to the house-keeping gene, β-actin. Qualitatively, all cytokine mRNA expression was detected in samples isolated from adherent cells present on all surfaces tested.

As shown in Figure 2, IL-1β expression by biomaterial adherent monocytes/macrophages did not

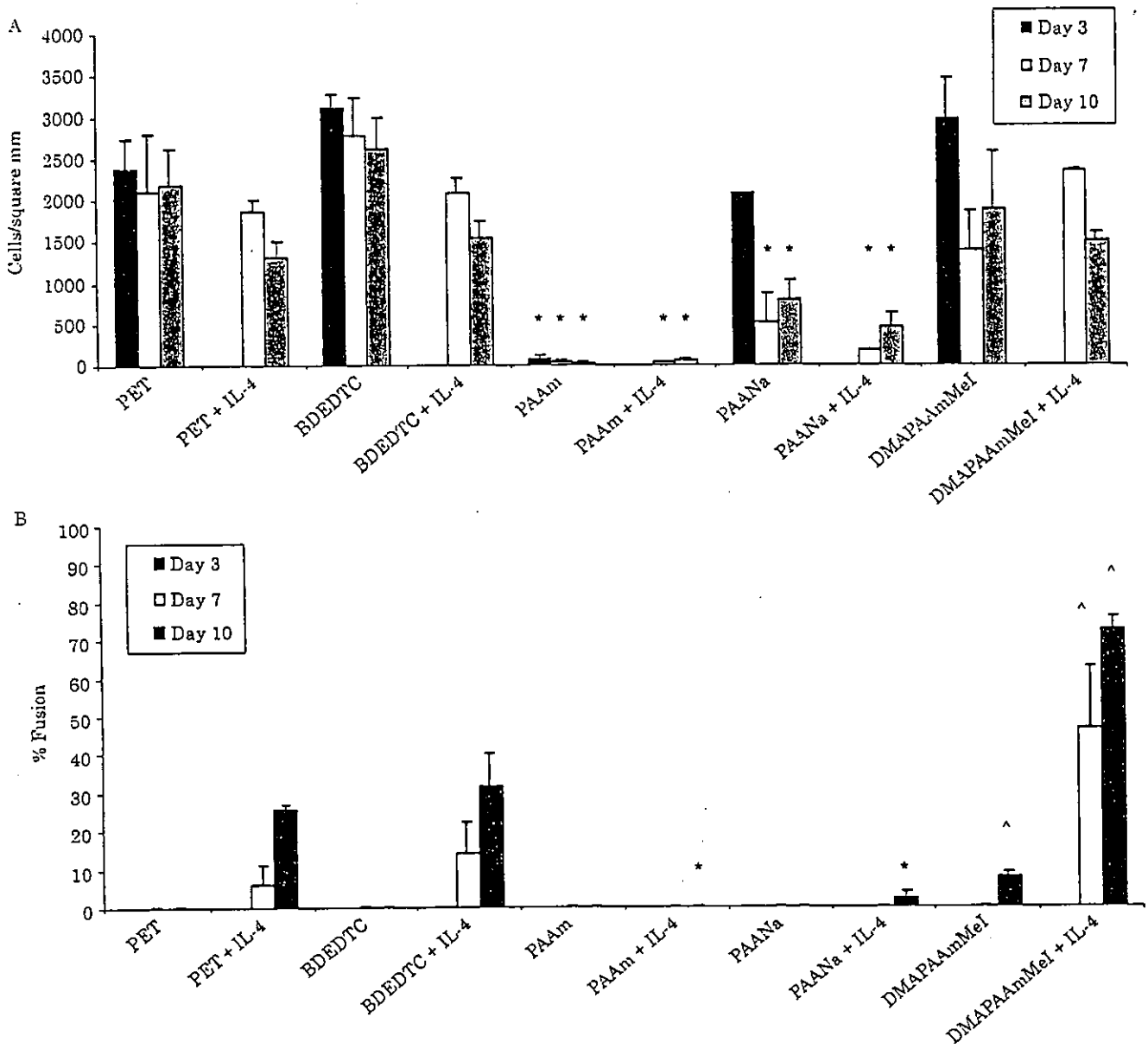

Figure 1. Adherent cell densities and fusion rates.

Adherent cells were fixed with methanol and stained with May Grünwald/Giemsa at the indicated times. (A) Cell densities were determined from counting 5–20 × objective fields for each sample and are expressed as cells/mm^2. (B) Fusion rates were determined by counting the number of nuclei within giant cells and dividing by the total number of nuclei in the given field and was repeated for 3–20 × objective fields. Data represent mean ± SEM, $n=5$. *Indicates significantly decreased values, and ^indicates significantly increased values when compared to the PET base surface where $P<0.05$.

vary among the different chemistries of the surface of adhesion nor with time, indicating time and surface independent levels of cell activation. Surprisingly, the expression ratios were also independent of the cell densities or rates of macrophage fusion (Fig. 1A and B, respectively). This was evident for the PAAm and PAANa surfaces that significantly promoted decreased rates of adhesion and fusion. Similar results were observed for TNF-α and IL-6 expression (data not shown). Notably, the addition of the Th_2/wound healing cytokine, IL-4, did not influence IL-1β expression levels.

Although no differences were observed in the expression ratios of IL-1β, its antagonist, IL-1RA, displayed a reduced surface-dependent expression (Fig. 3). In the presence of IL-4, monocytes and macrophages adherent to DMAPAAmMeI surfaces expressed significantly lower levels of IL-1RA when compared to all other surfaces ($P \leq 0.013$) on day 10 of culture. Once again, expression ratios did not correlate

CYTOKINE, Vol. 18, No. 6 (21 June, 2002: 311–319)

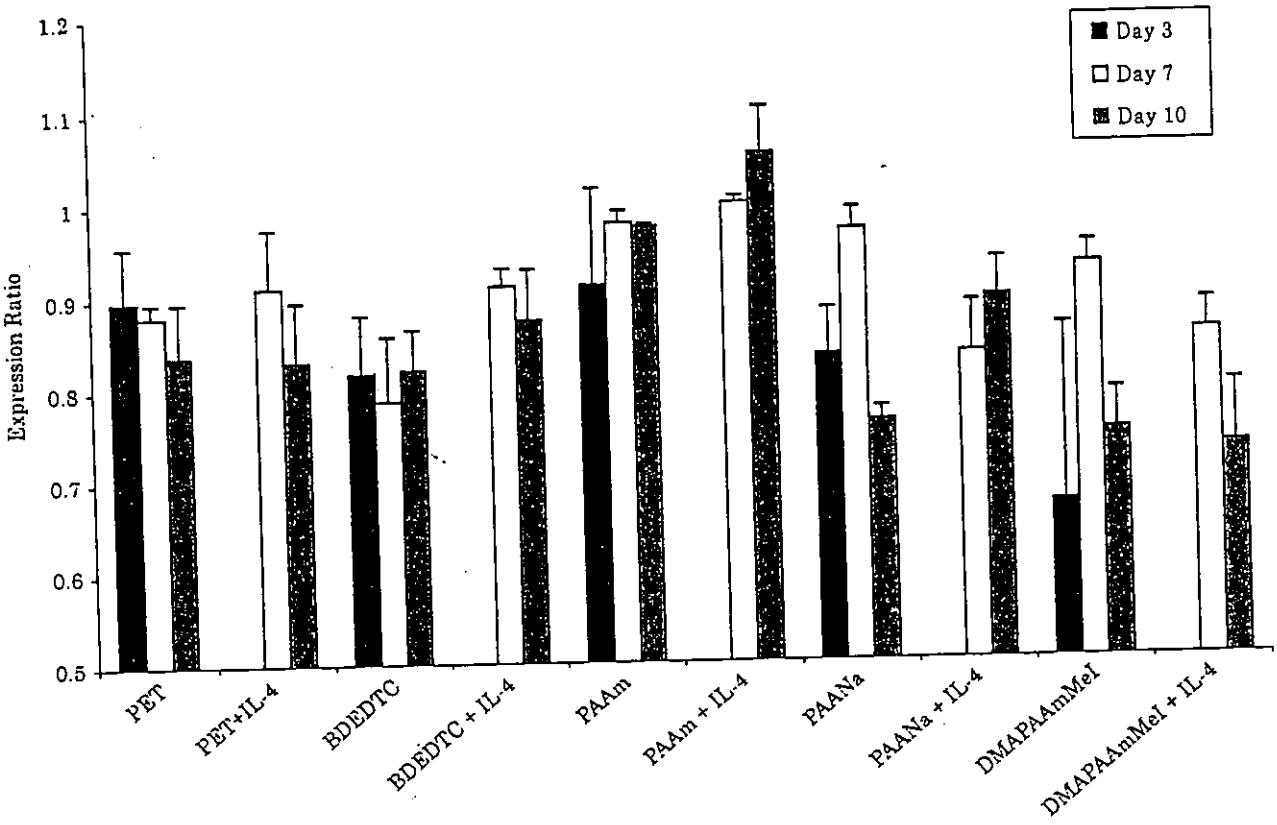

Figure 2. IL-1β expression by adherent cells.

Total RNA was isolated from duplicate culture wells and reversibly transcribed at the indicated time points under the given conditions. The IL-1β mRNA sequence was amplified by PCR, separated by electrophoresis and visualized by UV. Intensity of the bands was then quantified using SigmaScanPro with the digitized gel image. The intensity of each IL-1β band was divided by the corresponding β-actin band and results are presented as expression ratios. Data represent mean ± SEM, $n \geq 3$.

with cell surface densities. However, the decrease in IL-1RA expression did coincide with an increase of IL-4-dependent macrophage fusion on day 10 (Fig. 1B).

Unlike IL-1β, IL-6, TNF-α or IL-RA, IL-10 expression was dramatically influenced by substrate chemistry (Fig. 4). When compared to all surfaces tested, PAAm and PAANa surfaces promoted significantly increased levels of IL-10 expression ($P \leq 0.048$), while DMAPAAmMeI surfaces promoted significantly decreased adherent monocyte/macrophage expression of IL-10 on day 10 ($P \leq 0.047$). These differences occurred in conjunction with decreased rates of monocyte/macrophage adhesion and macrophage fusion on PAAm and PAANa surfaces and increased fusion rates on DMAPAAmMeI surfaces.

IL-8 expression showed an opposing pattern to that of IL-10 (Fig. 5). On day 10 of culture, biomaterial adherent monocyte/macrophage IL-8 expression was significantly decreased in cells adherent to the PAAm surface in the presence or absence of IL-4 as compared to all other surfaces ($P \leq 0.028$). Expression was also significantly decreased in cells adherent to the PAANa surface in the presence of IL-4 on day 10 of culture ($P \leq 0.027$). These decreased rates of IL-8 expression occurred in conjunction with decreased rates of monocyte/macrophage adhesion and macrophage fusion (Fig. 1A and B). The decreased expression of IL-8 on PAANa (Fig. 5), and the decrease of expression of IL-1RA on DMAPAAmMeI on day 10 (Fig. 3) are the only IL-4-dependent cytokine expression influences observed in these studies.

DISCUSSION

To determine whether biomaterial surface chemistry influences the types and/or levels of adherent monocyte/macrophage cytokine expression, we used our previously established human monocyte culture protocol in conjunction with semi-quantitative RT-PCR. We determined expression levels of IL-1β, TNF-α, IL-6, IL-8, IL-10 and IL-1RA produced by cells adherent to slightly hydrophobic (PET), hydrophobic (BDEDTC), hydrophilic (PAAm), anionic (PAANa) and cationic (DMAPAAmMeI) biomaterial surfaces. We found that IL-1β, TNF-α and IL-6 expression levels remained relatively unchanged among

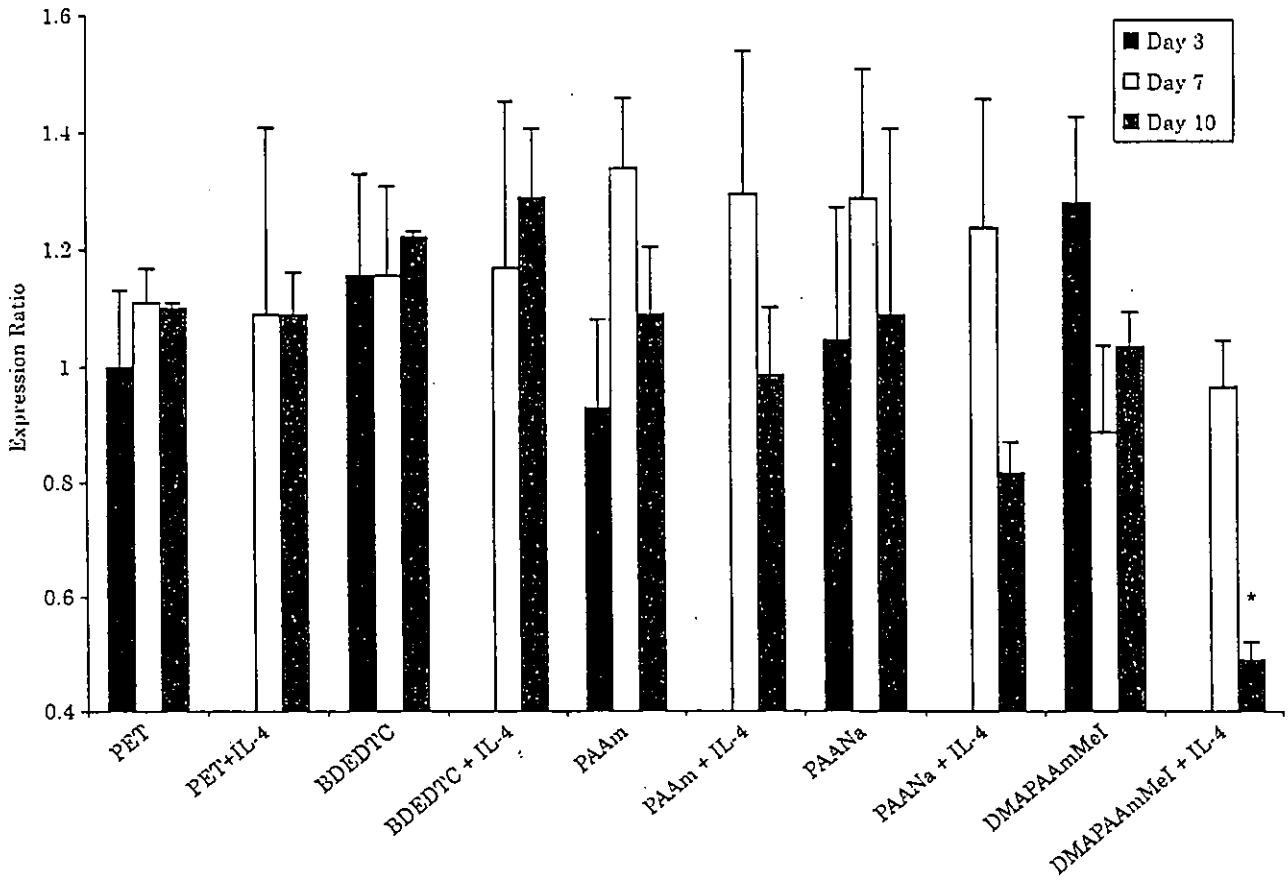

Figure 3. IL-1RA expression by adherent cells.

Total RNA was isolated from duplicate culture wells and reversibly transcribed at the indicated time points under the given conditions. The IL-1RA mRNA sequence was amplified by PCR, separated by electrophoresis and visualized by UV. Intensity of the bands was then quantified using SigmaScanPro with the digitized gel image. The intensity of each IL-1RA band was divided by the corresponding β-actin band and results are presented as expression ratios. Data represent mean ± SEM, $n \geq 3$. *Indicates significantly decreased expression ratio ($P < 0.05$).

cells adherent to any of the surface chemistries. However, DMAPAAmMeI surfaces promoted decreased levels of monocyte/macrophage IL-10 and IL-1RA expression while PAAm and PAANa surfaces promoted increased production of IL-10 and decreased production of IL-8 by adherent cells.

All biomaterial adherent monocytes and macrophages used in these studies expressed detectable levels of IL-1β, TNF-α, IL-6, IL-8, IL-10 and IL-1RA, indicating similar levels of cellular activation regardless of the surface of adhesion. Many studies examining cytokine production by immune cells induce monocyte/macrophage activation through stimulation by lipopolysaccharide (LPS) or other inflammatory agents. However, the presence of such agents may not only proportionately increase all cytokine levels, but also influence the types of cytokines being expressed, leading to misinterpretation of the data. Therefore, in these studies, we refrained from using inducing agents to directly assess the effects of surface chemistry on adherent monocyte/macrophage cytokine production.

Although adherent monocytes and macrophages maintained relatively constant expression levels of the cytokines among the different substrate surface chemistries, IL-8 and IL-10 expressions were significantly influenced by hydrophilic and anionic surface chemistries. IL-8 is most noted for its chemoattractant capabilities (reviewed in[18]). A decrease in monocyte/macrophage IL-8 production would lead to a decrease of chemotaxis of leukocytes to the site of the implant. IL-10 is responsible for decreasing cellular activity by inhibiting cytokine expression by a variety of cell types. Therefore, an increase of IL-10 production would indicate an overall suppression in the response to the implanted device. Taken together, the decrease in IL-8 production and increase in IL-10 production should decrease the overall response to the implant and therefore render the implant more biocompatible by decreasing the intensity of the foreign body response. It is also interesting to note that hydrophilic and anionic surfaces that promote such a response also increase rates of apoptosis of biomaterial adherent macrophages as well as decrease adhesion and fusion rates.[17]

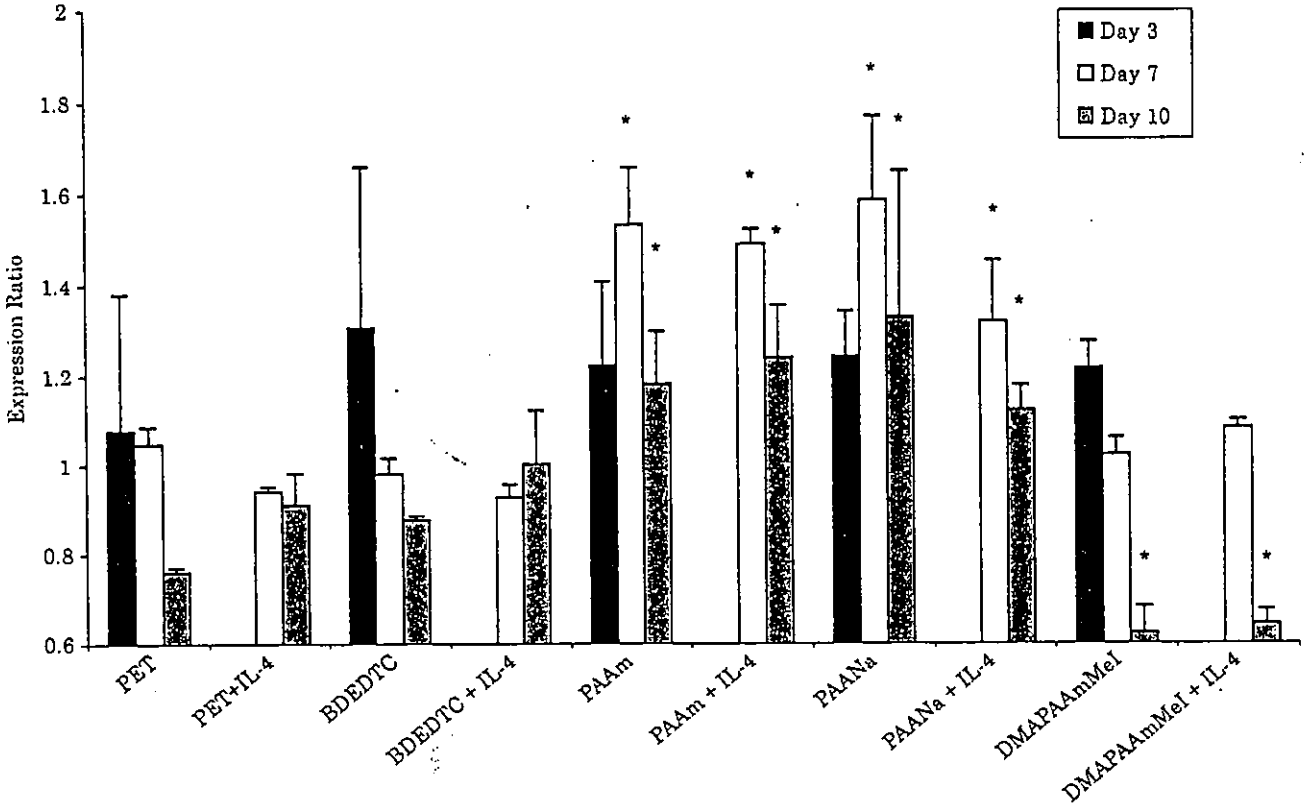

Figure 4. IL-10 expression by adherent cells.

Total RNA was isolated from duplicate culture walls and reversibly transcribed at the indicated time points under the given conditions. The IL-10 mRNA sequence was amplified by PCR, separated by electrophoresis and visualized by UV. Intensity of the bands was then quantified using SigmaScanPro with the digitized gel image. The intensity of each IL-10 band was divided by the corresponding β-actin band and results are presented as expression ratios. Data represent mean ± SEM, $n \geq 3$. *Indicates significantly increased or decreased expression ratios ($P<0.05$).

DMAPAAmMeI surfaces promoted decreased rates of IL-1RA and IL-10 adherent macrophage expression. A decrease in IL-1RA expression would lead to a greater susceptibility to IL-1β activation since IL-1RA's primary role is to act as an antagonist to IL-1β. In the in vivo environment, this may lead to an overall increase in cellular activation of cells involved in the inflammatory and wound healing responses. Additionally, the decrease in monocyte/macrophage IL-10 secretion would prevent the suppression of further activation and cytokine production. This suggests that cationic surfaces promote a more active response to the implanted material, promoting an inflammatory response, which may negatively impact biocompatibility. It is also important to note that fusion was greatest on these surfaces in these and other studies.[17] We have previously suggested that fusion of macrophages to form FBGCs acts as a mechanism to promote cell survival by escaping apoptosis.[19] The fusion may promote a more active response to the implant, suggesting an additional role of FBGCs to that of their classical role in the foreign body response. Since fusion coincides with decreased IL-1RA and IL-10 production it may have a cause-effect relationship. However, there is little known concerning the molecular or phenotypical differences between macrophages and FBGCs, and more direct evidence (such as in situ hybridization or immunohistochemical analysis) will be necessary to more clearly identify the source of the secreted cytokines.

The interaction of cells with the implant surface is not direct but mediated through an adsorbed protein layer that forms immediately. The levels of particular proteins adsorbed to a surface are dependent upon the surface chemistry.[13] This further leads to modulation of monocyte adhesion, macrophage activation and apoptosis. Monocytes adhere to the adsorbed protein layer through interactions with cell surface integrins.[20] Therefore, it is likely that these types of interactions are also responsible for determining cytokine expression by adherent cells, linking surface chemistry to selective cytokine expression by adherent cells.

The predominant Th_2 cytokine, IL-4, has been previously shown to induce macrophage fusion in vitro[10] and in vivo[11] and was therefore incorporated into these studies to induce fusion and observe any effects on cytokine production by adherent cells. Surprisingly, the presence of IL-4 in the cultures did not

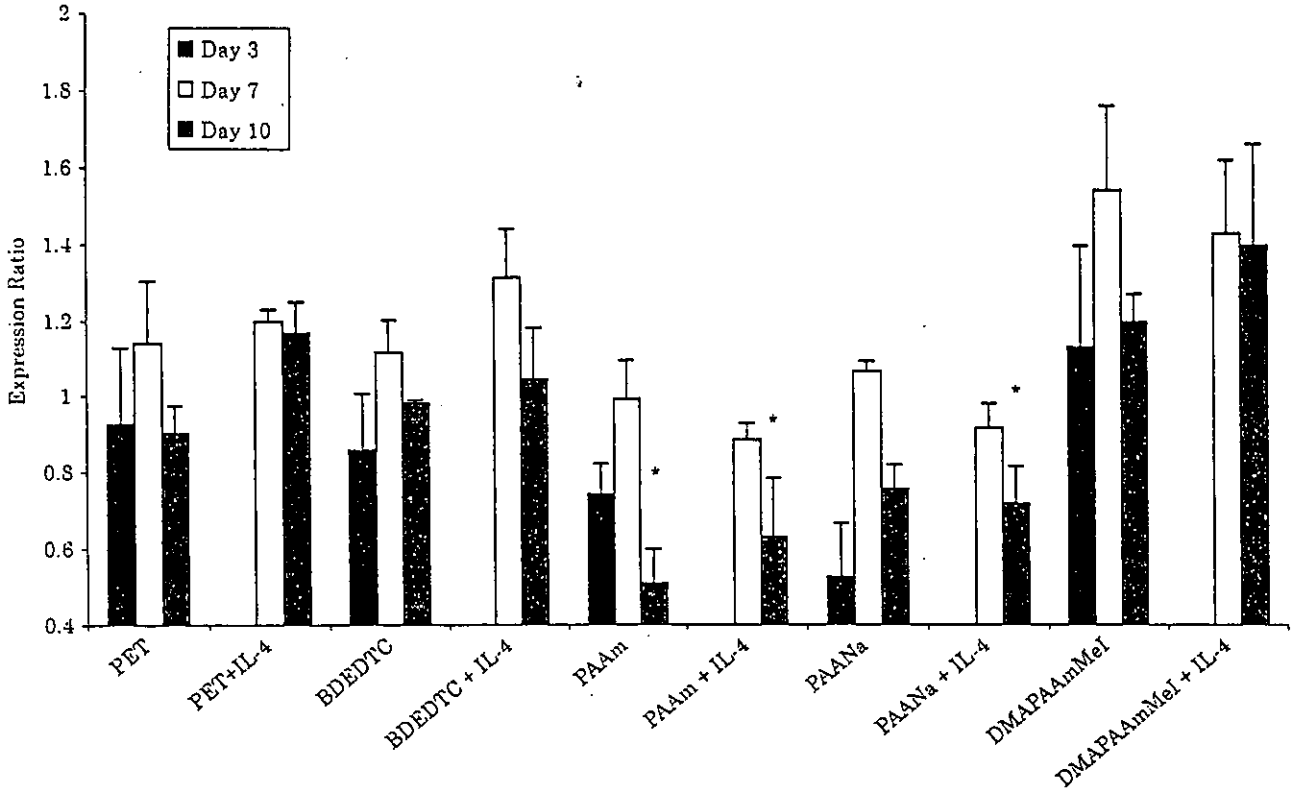

Figure 5. IL-8 expression by adherent cells.

Total RNA was isolated from duplicate culture wells and reversibly transcribed at the indicated time points under the given conditions. The IL-8 mRNA sequence was amplified by PCR, separated by electrophoresis and visualized by UV. Intensity of the bands was then quantified by using SigmaScanPro with the digitized gel image. The intensity of each IL-8 band was divided by the corresponding β-actin band and results are presented as expression ratios. Data represent mean ± SEM, $n \geq 3$. *Indicates significantly decreased expression ratios ($P<0.05$).

significantly change monocyte/macrophage cytokine expression except for a decrease of expression of IL-8 by PAANa adherent cells and IL-1RA by DMAPAAmMeI adherent cells. This suggests that the presence of Th_2 lymphocytes, secreting IL-4 around the implant should not influence the cytokines expressed by biomaterial adherent macrophages. The role of T cells in promoting selective biomaterial adherent monocyte/macrophage cytokine expression is an important line of research and we have recently shown that biomaterial surface chemistry affects the types and levels of lymphocyte cytokine expression in vivo (unpublished observations). The monocyte/macrophage interaction with the biomaterial surface and the resulting cytokine responses may affect the activity and cytokine expression of surrounding exudate cells resulting in surface chemistry-dependent lymphocyte cytokine production. On the other hand, lymphocytes may directly interact with the biomaterial surface[21–23] which may influence the levels and types of lymphocyte cytokine production, which then may modulate monocyte/macrophage adhesion, fusion and apoptosis.

Modulation of the foreign body response to implanted medical devices and prostheses is necessary to increase their biocompatibility. Essential components of this response are the monocyte and macrophage-derived cytokines that promote inflammation or wound healing. Therefore, influencing the types and levels of cytokines produced by biomaterial adherent cells is a feasible mechanism to confer biocompatibility to implants. Surface modification of the substrate provides a starting point to dictate adherent monocyte/macrophage cytokine production. These studies demonstrate that hydrophilic and anionic surfaces promote a predominant wound healing response while cationic studies promote a pro-inflammatory response.

MATERIALS AND METHODS

Surface preparation

Surfaces displaying distinct surface chemistries were prepared with a custom-designed, semiautomatic apparatus for laboratory-scale mass production as previously described.[24,25] PET film was coated with BDEDTC and photograft copolymerized with either PAAm, PAANa or DMAPAAmMeI. This provided slightly hydrophobic, hydrophobic, hydrophilic, anionic and cationic surfaces

CYTOKINE, Vol. 18, No. 6 (21 June, 2002: 311-319)

TABLE 1. Cytokine specific primers

Amplified RNA	Primer sequences (5'-3')	Size of amplified product (bp)	Reference
IL-1β	ATGGCAGAAGTACCTGAGCTCGCC GCTTTTTTGCTGTGAGTCCCGGA	474	(27)
TNF-α	CAGAGGGAAGAGTTCCCCAG CCTTGGTCTGGTAGGAGACG	325	(28)
IL-6	CAGCCACTCACCTCTTCAGAAC TGCAGGAACTGGATCAGGAC	332	(28)
IL-8	CTTGGCAGCCTTCCTGATTT CTCAGCCCTCTTCAAAAACT	256	(29)
IL-10	ATGCTTCGAGATCTCCGAGA AAATCGATGACAGCGCCGTA	269	(30)
IL-1RA	CTTCTATCTGAGGAACAACC TCATCACCAGACTTGACACA	158	(31)
β-actin	TACAATGAGCTGCGTGTGGCTCCCG AATGGTGATGACCTGGCCGTCAGGC	395	(32)

respectively.[17,25] Each surface was cut into 1.5 mm in diameter discs and inserted into the wells of 24-well plates following sterilization by brief ethanol rinsing. Surfaces were secured by silicone rubber rings (which were autoclaved prior to use), yielding an available surface area of 71.2 mm^2.

In vitro human monocyte culture

Whole blood was collected in the presence of 0.4% Sodium Citrate (Sigma, St. Louis, MO, USA) from nonmedicated, healthy adult volunteers. Human peripheral blood monocytes were isolated by a nonadherent density centrifugation method as previously described.[26] The cell culture medium consisted of RPMI-1640 supplemented with 20% autologous human serum and anti-biotic/anti-mycotic. Isolated monocytes were plated at a concentration of 5×10^5/ml in 1 ml for duplicate surfaces. Following a 2 h incubation at 37°C, surfaces were rinsed once with sterile PBS to remove any non-adherent cells and the media replaced. Media were replaced on days 3 and 7, containing 10 ng/ml IL-4 (Sigma) where noted.

Determination of cell densities and fusion rates

Adherent cell densities and macrophage fusion to form FBGCs were determined following staining by May Grünwald/Giemsa. Surfaces were rinsed with PBS twice and adherent cells were fixed by the addition of methanol for 5 min. Cells were then washed with PBS and May Grünwald reagent was added for 1 min followed by another PBS wash. Giemsa reagent was added for 5 min followed by a final wash with dH_2O. Cell densities were determined from 5–20 × objective fields for each sample and are expressed as cells/mm^2. Percent fusion was calculated by dividing the number of nuclei contained within giant cells by total number of nuclei in the field of view. This was repeated for 3–20 × objective fields.

Semi-quantitative RT-PCR

To quantitatively assess cellular expression levels of cytokines, total RNA was isolated from adherent cells at the indicated time points using TRIZOL Reagent (Gibco BRL, Gaithersburg, MD, USA) according to the manufacturer's instructions. Briefly, surfaces were rinsed twice with PBS solution and 250 µl of TRIZOL was added to each well. Duplicate samples were combined to ensure sufficient amounts of RNA, yielding 500 µl of cell extract per surface per condition. The extract was allowed to stand for 10 min followed by centrifugation at 10 K rpm for 10 min after which the pellets were discarded. Supernatants containing RNA were then mixed with 100 µl chloroform and inverted repeatedly for 15 s followed by 3 min incubation and centrifugation for 15 min at 10 K rpm. The resulting aqueous layer was then combined with 300 µl of isopropanol and mixed thoroughly. RNA was then pelleted and washed with 75% ethanol in autoclaved water. RNA was then dissolved in 11 µl of autoclaved water by incubating at 55°C for 10 min.

Messenger RNA was reversibly transcribed by combining the dissolved total RNA with 1 µl oligo$(dT)_{12-18}$ primer (Gibco-BRL Life Technologies, Gaithersburg, MD) and incubating for 10 min at 70°C followed by a quick incubation on ice and brief centrifugation. A mixture of 4 µl 5 × first strand buffer, 2 µl 0.1 M DTT, and 1 µl of 10 mM dNTP mix was then added to the sample and incubated for 2 min at 42°C. Reverse transcription was then initiated by the addition of 1 µl (200 units) Superscript II (Gibco-BRL Life Technologies) and the reaction was incubated at 42°C. After 50 min, the reaction was inactivated by heating the mixture to 70°C for 15 min. The reversibly transcribed product was then stored at −70°C until used for PCR.

PCR was performed using a GeneAMP 9700 PCR System (PE Applied Biosciences). Five microliters of reversibly transcribed product was used for each PCR reaction. A mix of 10 µl 10 × PCR buffer, 3 µl 50 mM MgCl2, 2 µl 10 mM dNTP mix, and 1 µl Taq DNA polymerase (5 U/µl) (Gibco-BRL Life Technologies) were used per reaction tube. Autoclaved water was then used to bring each reaction volume to 100 µl. Primer pairs were added to a final concentration of 10 µM. The primer pairs used to amplify specific cytokine and β-actin sequences are listed in Table 1. The

amplification was then performed for 35 cycles (94°C for 30 s, 60°C for 30 s and 72°C for 30 s per cycle).

The resulting amplified products were separated by electrophoresis through 1.5% agarose and visualized by UV of the intercalated ethidium bromide. Photographs were then digitally scanned and using SigmaScanPro 4.0 the band intensities were quantified. Expression ratios were determined by dividing the band intensity of the product of interest by that of the corresponding β-actin band.

Statistics

All data are expressed as the average of at least three replicate experiments utilizing cells isolated from different donors ± the standard error of the mean. Statistical comparisons were performed using the Bonferroni/Dunn test, using StatView v4.1 (Abacus Concepts, Berkeley, CA, USA).

REFERENCES

1. Sutton JS, Weiss L (1966) Transformation of monocytes in tissue culture into macrophages, epithelioid cells, and multinucleated giant cells. J Cell Biol 28:303–332.

2. Murch AR, Grounds MD, Marshall CA, Papadimitriou JM (1982) Direct evidence that inflammatory multinucleated cells form by fusion. J Pathol 137:177–180.

3. Kreipe H, Razdun HJ, Rudolph P, Barth J, Hansmann M, Heidorn K, Parwaresch MR (1988) Multinucleated giant cells generated in *in vitro*: Terminally-differentiated macrophages with down-regulated c-myc expression. Am J Pathol 130:232–234.

4. McInnis A, Rennick DM (1988) Interleukin-4 induces cultured monocytes/macrophages to form multinucleated cells. J Exp Med 167:598–611.

5. Weinberg JB, Hobbs MM, Misukonis MA (1984) Recombinant human gamma-interferon induces human monocyte polykaryon formation. Proc Natl Acad Sci USA 81:454–457.

6. Hassan NF, Kamani N, Meszaros MM, Douglas SD (1989) Induction of multi-nucleated giant cell formation from human blood-derived monocytes by phorbol myristate acetate *in vitro* culture. J Immunol 143:2179–2184.

7. Anderson JM (1996) Implant retrieval and evaluation in biomaterials science: an introduction to materials in medicine. In: Ratner BD, Hoffman AS, Schoen FJ, Lemons JE (eds) Biomaterials Science. Academic Press, New York, pp 451–455.

8. Zhao Q, Topham N, Anderson JM, Lodoen G, Payet CR (1991) Foreign-body giant cells and polyurethane biostability: In vivo correlation of cell adhesion and surface cracking. J Biomed Mater Res 25:177–183.

9. Ziats NP, Miller KM, Anderson JM (1988) In vitro and in vivo interactions of cells with biomaterials. Biomaterials 9:5–13.

10. McNally AK, Anderson JM (1995) Interleukin-4 induces foreign body giant cells from human monocytes/ macrophages. Differential lymphokine regulation of macrophage fusion leads to morphological variants of multinucleated giant cells. Am J Pathol 147:1487–1499.

11. Kao WJ, McNally AK, Hiltner A, Anderson M (1995) Role for interleukin-4 in foreign-body giant cell formation on a poly(etherurethane urea) in vivo. J Biomed Mater Res 29:1267–1275.

12. Horbett TA (1993) Principles underlying the role of adsorbed plasma proteins in blood interactions with foreign materials. Cardiovasc Pathol 2:137S–148S.

13. Jenney C, Anderson J (2000) Adsorbed serum proteins responsible for surface dependent human macrophage behavior. J Biomed Mater Res 49:435–447.

14. DeFife KM, Yun JK, Azeez A, Stack S, Ishihara K, Nakabayashi N, Colton E, Anderson JM (1995) Adhesion and cytokine production by monocytes on poly(2-methacryloyloxyethyl phosphorycholine-co-alkyl methacrylate)-coated polymers. J Biomed Mater Res 29:431–439.

15. DeFife KM, Hagen KM, Clapper DL, Anderson JM (1999) Photochemically immobilized polymer coatings: effects on protein adsorption, cell adhesion, and leukocyte activation. J BioMater Sci Polym Ed 10:1063–1074.

16. Nakaoka R, Tsuchiya T, Nakamura A (2000) Studies on the mechanisms of tumorigenesis induced by polyetherurethane in rats: Production of superoxide, tumor necrosis factor, and interleukin 1 from macrophages cultures on different polyetherurethanes. J Biomed Mater Res 49:99–105.

17. Brodbeck WG, Shive MS, Colton E, Nakayama Y, Matsuda T, Anderson JM (2001) Influence of biomaterial surface chemistry on apoptosis of adherent cells. J Biomed Mater Res 55:661–668.

18. Matsushima K, Baldwin ET, Mukaida N (1992) Interleukin-8 and MCAF: novel leukocyte recruitment and activating cytokines. Chem Immunol 51:236–265.

19. Brodbeck WG, Shive MS, Colton E, Ziats NP, Anderson JM (2001) IL-4 inhibits apoptosis of biomaterial adherent monocytes/macrophages. J Lab Clin Med 139:90–100.

20. Anderson JM, DeFife KM, McNally AK, Collier TO, Jenney CR (1999) Monocyte, macrophage and foriegn body giant cell interactions with molecularly engineered surfaces. J Mater Sci: Mater Med 10:579–688.

21. Groth T, Zlatanov I, Altankov G (1994) Adhesion of human peripheral lymphocytes on biomaterials preadsorbed with fibronectin and vitronectin. J Biomater Sci Polym Ed 6:729–739.

22. Maeda M, Kimura M, Inoue S, Kataoka K, Okano T, Sakurai Y (1986) Adhesion behavior of rat lymphocyte subpopulations (B cell and T cell) on the surface of polystyrene/polypeptide graft copolymer. J Biomed Mater Res 20:25–35.

23. Tanaka T, Yamakawa N, Mizusawa T, Usui M (2000) Interaction between inflammatory cells and heparin-surface-modified intraocular lens. J Cataract Refract Surg 26:1409–1412.

24. Nakayama Y, Matsuda T (1996) Surface macromolecular architectural designs using photograft copolymerization based on photochemistry of benzyl N,N-diethyldithiocarbamate. Macromolecules 29:8622–8630.

25. DeFife KM, Colton E, Nakayama Y, Matsuda T, Anderson JM (1999) Spatial regulation and surface chemistry control of monocyte/ macrophage adhesion and foreign body giant cell formation by photochemically micropatterned surfaces. J Biomed Mater Res 45:148–154.

26. McNally AK, Anderson JM (1994) Complement C3 participation in monocyte adhesion to different surfaces. Proc Natl Acad Sci USA 91:10119–10123.

27. Harris PR, Smythies LE, Smith PD, Dubois A (2000) Inflammatory cytokine mRNA expression during early and persistent helicobacter pylori infection in nonhuman primates. J Infect Dis 181:783–786.

28. Barth S, Kleinhappl B, Gutschi A, Jelovcan S, Marth E (2000) In vitro cytokine mRNA expression in normal human peripheral blood mononuclear cells. Inflamm Res 49:266–274.

29. De Rossi M, Bernasconi P, Baggi F, de Waal Malefyt R, Mantegazza R (2000) Cytokines and chemokines are both expressed by human myoblasts: possible relevance for the immune pathogenesis of muscle inflammation. Int Immunol 12:1329–1335.

30. Csiszar A, Nagy GY, Gergely P, Pozsonyi T, Pocsik E (2000) Increased interferon-gamma (IFN-γ), IL-10 and decreased IL-4 mRNA expression in peripheral blood mononuclear cells (PBMC) from patients with systemic lupus erythematosus (SLE). Clin Exp Immunol 122:464–470.

31. Shimozato O, Watanabe N, Goto M, Kobayashi Y (1996) Cytokine production by SV40-transformed adherent synovial cells from rheumatoid arthritis patients. Cytokine 8:99–105.

32. Van Coillie E, Froyen G, Nomiyama H, Miura R, Fiten P, Van Aelst I, Van Damme J, Opdenakker G (1997) Human monocyte chemotactic protein-2: cDNA cloning and regulated expression of mRNA in mesenchymal cells. Biochem Biophys Res Commun 231:726–730.

Development of a Water-Soluble Matrix Metalloproteinase Inhibitor as an Intra-arterial Infusion Drug for Prevention of Restenosis after Angioplasty

Takeshi Masuda and Yasuhide Nakayama*

Department of Bioengineering, National Cardiovascular Center Research Institute, 5-7-1 Fujishiro-dai, Suita, Osaka 565-8565, Japan

Received August 19, 2002

To prevent restenosis after percutaneous transluminal coronary angioplasty (PTCA) and/or stenting of atherosclerotic stenosed arteries, we designed and developed two water-soluble matrix metalloproteinases (MMPs) inhibitors. The first inhibitor was monomeric in type and was chemically synthesized by succinylation of the synthetic MMP inhibitor, *N*-hydroxy-5-hydroxy-2(*S*)-methyl-4(*S*)-(4-phenoxybenzoyl)aminopentanamide (ONO-M11−335). The second inhibitor was polymeric and was a radical copolymer of the vinyl derivative of ONO-M11-335 and a water-soluble monomer, *N*,*N*-dimethylacrylamide (DMAAm). For the second inhibitor, NMR analyses and UV−vis spectra measurements showed that the content of the ONO-M11-335 unit in the copolymers (M_n; ca. 10 000 and 20 000 by GPC measurements) was about 8 per molecule. The MMP inhibitors were all highly soluble in water, even under neutral pH. The succinylated derivative markedly inhibited MMP-2, MMP-9, and MMP-12 in vitro, as did ONO-M11-335. In contrast the copolymers, which can maintain effective plasma levels for extended periods by prevention of hepatic uptake, showed a ca. 100-fold reduced inhibition activity. Such water-soluble MMP inhibitors, developed in this study, may potentially be useful as an intra-arterial infusion drug for vascular injury.

Introduction

Matrix metalloproteinases (MMPs) are classified into a series of the proteinase family and contain over 20 species of zinc-dependent endopeptidases.[1] The MMPs facilitate the degradation and remodeling of the extracellular matrix (ECM), including the interstitial and basement membranes, fibronectin, elastin, and laminin. The physiological role of the MMPs is to degrade ECM components, which promote connective tissue remodeling processes and which are expressed during the morphogenetic stage of embryonic development and differentiation, bone resorption, and tissue repair. The MMPs are also associated with various oncologic or pathological processes such as tumor invasion, rheumatoid joint destruction, uterine adenomyosis, and cardiovascular disease.[2]

In normal tissue, expression of MMP is regulated at the gene transcription level by extracellular stimulators[3] such as cytokines, growth factors, and cell or matrix−cell interactions. Once synthesized, they are secreted from cells as pre-proenzymes which can be activated by serine proteinases or other activated MMPs in the extracellular space.[4] In a defined activation mechanism, gelatinase A (MMP-2) is activated by interacting with a membrane type-1 MMP (MT1-MMP) that is activated preliminary by furin and by anchorage to the cell membrane surface.[5] The activity of MMP is inhibited by a natural tissue inhibitor of the metalloproteinase (TIMP), which is also secreted by transcriptional regulation and inhibit MMP activity by binding to the catalytic domain of the activated MMP.[6]

Percutaneous transluminal angioplasty in coronary and peripheral arteries (PTCA or PTA) has been widely used for clinical treatment of atherosclerotic stenosis using either balloon catheters or metallic stents. However, it has been reported that around 30−50% of restenosis cases have occurred few months after balloon angioplasty. Such a phenomenon remains an unsolved problem. One of the major causes of the restenosis was excessive tissue ingrowth (intimal hyperplasia), resulting from migration and proliferation of smooth muscle cells (SMC), and is triggered by degradation of the extracellular matrix by SMC derived MMP. MMP inhibitors therefore offer potential as a therapeutic tool for prevention of restenosis, and to this end, chemically synthesized MMP inhibitors have been widely developed over the past few decades.[7] X-ray crystallographic analyses of a single crystal of the MMP-inhibitor complex has been revealed together with determination of the enzyme's active site and the interaction mechanism between inhibitor and MMP.[8] Such information has been instrumental in the design of synthetic MMP inhibitors.[9] A number of MMP inhibitors, with varying efficiency, have been described which are involved in collagen peptidomimetics and nonpeptidomimetics.[10] These have been further classified according to the variety of their coordination groups binding to the zinc atom localized on the enzyme active site such as hydroxamate, phosphinate, thiol, and sulfodiimine. However, since most of these MMP inhibitors show extremely poor water solubility they are not maintained at high levels in the plasma, which is not suitable for an intra-arterial infusion drug.

In this study, we molecularly designed and developed two types of water-soluble MMP inhibitors by either derivatization of the carboxyl group or copolymerization

* To whom correspondence should be addressed. Tel: (+81) 6-6833-5012 (ext 2434). Fax: (+81) 6-6872-8090. E-mail: nakayama@ri.ncvc.go.jp.

10.1021/jm020356g CCC: $25.00
Published on Web 07/03/2003

Scheme 1. Synthetic Scheme of Water-Soluble Matrix Metalloproteinase Inhibitors

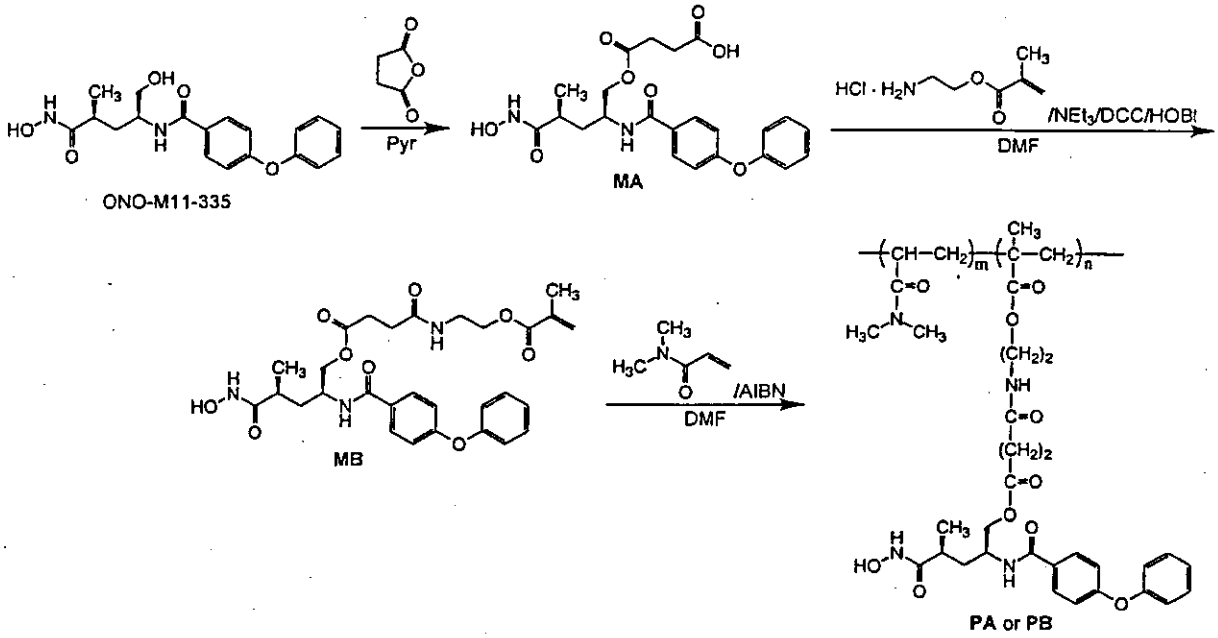

Table 1. Preparation of Poly(AEMA-ONO-*co*-DMAAm)

	feed of MB (mol %)	yield (%)	degree of derivatization of MB unit (mol %)		M_n ($\times 10^4$)	M_w/M_n	no. of MB units/molecule
			^{1}H NMR[a]	UV[b]			
PA	5	70	5.4	6.0	1.8	2.81	7.8
PB	10	81	9.8	9.1	1.1	3.73	7.4

[a] Calculated from integration value ratio of $-CH_3$ protons of DMAAm vs aromatic ring protons of AEMA-ONO. [b] All analytical samples are prepared as 0.2 mg/mL of EtOH solution and molarity of ONO-M11-335 contained in sample solution was estimated by the molar extinction coefficient of MB at 253 nm. The λ_{max} was not different from monomer and copolymers. [c] Calculated from ^{1}H NMR.

with a water-soluble monomer to enable water-solubility of the synthetic MMP inhibitor ONO-M11-335. As for the copolymers, controlled drug delivery by hydrolysis in vivo was predicted. The potential abilities of the MMP inhibitors for clinical applications in intra-vascular surgery including PTCA and stenting are discussed.

Results

Preparation of Water-Soluble MMP Inhibitors. Two different molecular designs were used for the water-solubilization of the synthetic MMP inhibitor ONO-M11-335 (Scheme 1). The first approach involved synthesis of a monomeric inhibitor (MA), whereas the second approach involved synthesis of a polymeric inhibitor (PA and PB).

The monomeric MMP inhibitor (MA) was synthesized by derivatization of a succinic acid moiety to the ONO-M11-335 through an ester bond. The esterification of ONO-M11-335 was performed by nucleophilic attack of the 5-OH group of ONO-M11-335 to the carbonyl group of succinic anhydride in anhydrous pyridine at room temperature. The unfavorable nucleophilic attack of the nonprotected OH group of the hydroxamate moiety was preferentially prevented to minimize production of an amide derivative being negative to hydroxamic acid method.

The polymeric inhibitors (PA and PB) were synthesized by copolymerization of DMAAm with a vinyl derivative of ONO-M11-335 (MB) by an amide bond formation between MA and 2-aminoethyl methacrylate using DCC–HOBt as the coupling reagent. The amide bond procedure proceeded quantitatively with little side reactions or formation of byproducts resulting from the hydroxamate group. Thereafter, the ONO-M11-335 appending vinyl monomer (MB) was polymerized with DMAAm, in the presence of AIBN, as a conventional radical polymerization initiator (Scheme 1). Table 1 summarizes the composition of the obtained copolymers. The molecular weight of the copolymers (PA and PB) was around 20 000 and 10 000, respectively. The degree of derivatization of the MB unit in the copolymers was calculated using two alternative methods. The first method calculated the value from the ratio of the integrals of the aromatic ring protons ($\delta = 7.0-7.8$ ppm) of the MMP inhibitor unit with the dimethyl amide protons ($\delta = 2.6-3.4$ ppm) of the DMAAm unit in the ^{1}H NMR spectra. The second method determined the value from the UV/vis absorption spectrum of the copolymers using the absorption coefficient of the MB, which has a maximum absorption at a wavelength of 253 nm in ethanol ($\epsilon = 16\,230$). There was good agreement between the copolymer compositions calculated from ^{1}H NMR spectra and from UV/vis spectra. The degree of derivatization of MMP inhibitor unit in the copolymers was around 5 mol % (PA) and 10 mol % (PB), respectively. Thus, the number of the inhibitor unit in the two copolymers was about 8 per molecules. The succinylated derivative (MA) and two copolymers

Table 2. Solubility of MMP Inhibitors in Various Aqueous Solutions

	solubility (μg/mL)		
MMP inhibitor	artificial bile	buffer (pH 7.4)	purified water
ONO-M11-335	432	307	372
MA	>1000	>1000	398
PA	>1000	>1000	
PB	>1000	>1000	

Table 3. Human Matrix Metalloproteinase Inhibition Activities

	IC_{50} value (nM)[a]		
MMP inhibitor	MMP-2	MMP-9	MMP-12
ONO-4817	0.73	2.10	0.45
ONO-M11-335	0.65	0.80	3.50
MA	1.10	2.80	2.60
PA[b]	50	83	120
PB[b]	100	200	260

[a] 50% inhibitory concentration. [b] Exact molecular weights of polymers were not clear; however, their molar concentration was determined by a net inhibitor ratio involved in each polymers and number-average molecular weight estimated from GPC.

(**PA** and **PB**) were all very soluble in water even under neutral pH (Table 2).

Inhibition Activity for Human Matrix Metalloproteinase. ONO-M11-335 was a highly potent and relatively selective MMP inhibitor for MMP-2 and gelatinase B (MMP-9) compared with MMP-1 or MMP-7. The IC_{50} values (50% inhibitory concentration) for MMP-2, MMP-9, and MMP-12 (metalloelastase) were 0.65, 0.80, and 3.50 nM, respectively (Table 3). MA also showed high MMP inhibition activities comparable to ONO-M11-335, with IC_{50} values for MMP-2, MMP-9, and MMP-12 of 1.10, 2.80, and 2.60 nM, respectively. The IC_{50} values of MMP inhibitor-DMAAm copolymers for MMP-2, MMP-9, and MMP-12 were also estimated and were revealed to be 100, 200, and 260 nM for **PA** and 50, 83, and 120 nM for **PB**.

Discussion

Both vascular constructive remodeling and neointimal hyperplasia are major causes of restenosis in response to arterial injury after balloon angioplasty. In stenting, the possibility of constructive remodeling is almost excluded. It has, however, been reported that 20−30% of in-stent restenosis cases are observed a few months after stenting, which may be mainly due to neointimal hyperplasia, triggered by early SMC migration to the luminal surface of the artery after angioplasty injury and followed by SMC proliferation and ECM production. Therefore, one of the therapeutic strategies for the prevention of restenosis is the suppression of SMC migration using immunosuppressive agents such as FK506 and Rapamycin.[11] Both these agents bind to the cytosolic receptor. For instance, FK506 binds to FKBP12, which is physically associated with the type I TGF-β receptor and inhibits the SMC migration by blocking the growth factor mediated signal transduction pathways. Recent reports have shown that stents coated with these agents possessed sustained release from the polymer matrix and resulted in remarkably reduced in-stent restenosis.[12]

On the other hand, recent studies on the pathology of restenosis have focused on the role of ECM, which is concerned with structure and function, and the importance of the vascular ECM for the vascular reconstruction response to arterial injury, such as balloon and/or stent angioplasty. ECM degradation, which has a central role in SMC migration and proliferation during the early stages of neointimal hyperplasia, depends on a group of proteases known as MMPs. In mechanical arterial injury, overexpression of various MMPs, including stromelysin (MMP-3), collagenases (MMP-1), and gelatinases (MMP-2 and MMP-9) occurs during SMC migration.

Many different types of synthetic MMP inhibitors have been developed and assessed in clinical trials. For example marimastat,[13] a synthetic hydroxamate type MMP inhibitor, mimics the structure of collagen at the site where MMP binds to the zinc ion, which is located at the active site of the MMP and is held in a stereospecific manner. Marimastat is widely known to inhibit the activity of MMP-1, -2, -3, -7, and -9 but possesses a relatively nonspecific selectivity for the MMPs. Other peptide-mimetic hydroxamic acid type MMP inhibitors include GM 6001.[14] developed by Glycomed, Inc., which has been studied for its SMC antiproliferation activity in SMC migration assays and has been found to almost completely inhibit SMC migration, without reducing the number of cells available to migrate from the media to intima. On the other hand, ONO-4817,[15] a novel hydroxamic acid-based nonpeptide type orally active synthetic MMP inhibitor, was developed in ONO Pharmaceutical Co., which shows a broad inhibitory activity against MMPs except MMP-1 and MMP-7 at nanomolar concentration levels.

In contrast, our group developed a new percutaneous transluminal coronary angioplasty catheter with multiple functions for balloon inflation, local drug delivery, and coronary perfusion.[16−18] Water-soluble drugs can be infused from a port located distal to the inflated balloon during continuous blood perfusion via the perfusion lumen. Recently, local administration of several agents, including hepatocyte growth factor, docetaxel,[17] and a C-type natriuretic peptide,[18] directly to the injured site has attracted increasing interest as a potential therapeutic method for the prevention of restenosis.[19] Local drug delivery may allow a sufficient concentration of the drug to be achieved at tissue while minimizing systemic adverse effects. To use in intra-arterial infusion drug, water solubility is necessary. The synthetic works have been done for the design of water-soluble. For example, Scozzafava et al. synthesized water-soluble sulfonamides by attaching water-solubilizing moieties such as pyridine carboximide, carboxypyridinecarboxamide, etc., in which carbonic anhydrase inhibitors derivatized with water-soluble tail structure showed topical activity as an antiglaucoma drug.[20] In this study, we first designed two alternative approaches for water solubilization of the MMP inhibitor ONO-M11-335 by applying simple chemical reactions. As expected, both MMP inhibitors were highly soluble in water even under neutral pH (Table 2). The first inhibitor, which is monomeric succinate derivative (MA), can potentially acquire high doses at local areas using the above-mentioned multiple functional balloon catheter. On the other hand, the second inhibitor, which is copolymer with *N,N*-dimethylacrylamide (PA and PB), can potentially acquire an